Research Square

Preprints are preliminary reports that have not undergone peer review.
They should not be considered conclusive, used to inform clinical practice,
or referenced by the media as validated information.

Opposing genetic pathways link obesity to depression through distinct circulating proteins and brain phenotypes

Haozhang Huang

1017988724@qq.com

Southern Medical University https://orcid.org/0000-0001-7524-2854

Ming Chen

the Third Affiliated Hospital of Sun Yat-sen University

Shuo Zheng

Weipeng Zhang

Jian Mao

Huangtao Ruan

Yong Liu

Cai-Lan Hou

Guangdong Provincial People's Hospital (Guangdong Academy of Medical Sciences)

Shiqun Chen

Article

Keywords: obesity, depression, Mendelian randomization, genetic clustering, plasma proteome, neuroimaging, polygenic risk score

Posted Date: November 4th, 2026

DOI: https://doi.org/10.21203/rs.3.rs-11032348/v1

License: This work is licensed under a Creative Commons Attribution 4.0 International License.
Read Full License

Additional Declarations: The authors have declared there is **NO** conflict of interest to disclose

Abstract

Obesity and depression frequently co-occur, and evidence supports a causal relationship. However, obesity is heterogeneous, and its genetic components may exert divergent, even opposing, effects on depression risk. We clustered BMI-associated single-nucleotide polymorphisms (SNPs) based on their Mendelian randomization (MR) estimates on depression risk and validated each cluster using cluster-specific polygenic risk scores (PRS) in the UK Biobank (N = 457,929). Two-step MR was used to assess whether circulating proteins and brain imaging-derived phenotypes (IDPs) mediated the cluster-specific effects. Four SNP clusters associated with elevated BMI showed differential associations with depression risk: C1 (high-risk) and C2 (moderate-risk) were associated with increased risk, C3 exerted a protective effect, and C4 showed no robust association. In the UK Biobank, C1-PRS (OR = 1.67, 95% CI = 1.56–1.79) and C2-PRS (OR = 1.25, 95% CI = 1.16–1.35) were associated with increased depression risk, whereas C3-PRS was associated with decreased risk (OR = 0.78, 95% CI = 0.71–0.88). Two-step MR identified ANGPTL2, MEP1B, and VWC2L as shared circulating mediators of C1 and C2, with PHLDB1 specific to C1, whereas FURIN, HLA-E, HSPB6, and PARP1 mediated the protective C3 effect. rfMRI connectivity (ICA100 edge 73) and right putamen signal intensity mediated the C1 (1.8%, P = 0.045) and C3 (2.1%, P = 0.014) pathways, respectively. Obesity influences depression risk through distinct, even opposing, genetic pathways mediated by specific circulating proteins and neuroimaging phenotypes, highlighting potential targets for subtype-specific intervention.

INTRODUCTION

Depression is a leading contributor to the global burden of disease, with a complex etiology involving intricate interactions among genetic, environmental, and metabolic factors [1–3]. Obesity, a well-established risk factor for a range of brain-related disorders, has been consistently associated with an elevated risk of depression [4–6]. However, emerging evidence suggests that being underweight may also independently contribute to depression risk [7–9].

Circulating plasma proteins reflect complex biological signaling networks that traverse multiple tissues and organ systems, and may directly participate in or regulate the pathogenesis of complex diseases, including both obesity and depression [10–12]. In parallel, individuals with obesity and those who are underweight have been shown to exhibit distinct neuroanatomical profiles [4,13], and certain structural brain alterations have been linked to depression [14]. Collectively, these findings suggest that body mass index (BMI) may influence depression risk through at least two potential biological pathways: alterations in the plasma proteome and/or changes in brain structure. Nevertheless, systematic studies directly linking BMI, the plasma proteome, and brain structural phenotypes to depression remain scarce, particularly when accounting for the heterogeneity of BMI that is, the possibility that high and low BMI may influence depression risk through distinct causal mechanisms.

In this study, we leveraged Mendelian randomization (MR) together with data from a large prospective cohort to systematically dissect the causal pathways linking BMI to depression, integrating genetic

clustering, plasma proteomics, and brain imaging-derived phenotypes (IDPs) to identify potential biological mediators and biomarkers.

METHODS

Study Design

This study comprised three sequential analytical steps, leveraging large-scale individual-level data and genome-wide association study (GWAS) summary statistics (Fig. 1). First, to identify genetic variants representing distinct mechanistic pathways linking BMI to depression, we applied a clustering-based Mendelian randomization (MR) approach—MR-Clust—based on the effects of BMI-associated variants on depression risk [15,16]. Second, we validated cluster-specific effects in the UK Biobank cohort using cluster-specific BMI polygenic risk scores (PRS). Third, we performed two-step MR analyses to assess whether cluster-specific BMI-associated SNPs influenced depression risk through circulating proteins and brain imaging-derived phenotypes (IDPs). The study followed the STROBE-MR guidelines [17,18].

GWAS Data sources and cluster meta-analysis for BMI and depression

Summary statistics for BMI (primary exposure) were obtained from a combined meta-analysis of the Genetic Investigation of Anthropometric Traits (GIANT) Consortium, comprising up to 681,275 individuals of European descent [19]. Summary statistics for depression were derived from the most recent Psychiatric Genomics Consortium (PGC) GWAS meta-analysis (N = 1,639,572; 357,636 cases, 1,281,936 controls), excluding UK Biobank and 23andMe samples to avoid sample overlap [20]. All instrumental variables (IVs) were required to satisfy the three core MR assumptions—relevance, independence, and exclusion restriction—with quality control implemented accordingly.

Quality control was performed using the TwoSampleMR R package. Non-biallelic and non-inferable palindromic SNPs were excluded, and the two datasets were harmonized such that the effect of each allele was consistently estimated across both phenotypes. Proxy SNPs were not used. Steiger filtering was applied to exclude SNPs for which the proportion of variance explained in depression exceeded that explained in BMI, thereby removing variants for which the direction of causality could not be confidently assumed to run from BMI to depression. Following harmonization and Steiger filtering, the remaining genome-wide significant, independent SNPs were carried forward for clustering analysis using MR-Clust. All MR analyses and other statistical tests were performed using R version 4.5.1.

To identify SNP clusters representing distinct biological pathways linking obesity to depression, we applied the MR-Clust algorithm (MR-Clust R package), which classifies genetic variants based on their effects on BMI and depression risk using GWAS summary statistics. The algorithm fits a mixture model in which ratio estimates follow cluster-specific normal distributions for substantive clusters or a high-

variance distribution for the "junk" (null) cluster. Cluster means (θ) and mixture proportions (π) were estimated using an expectation-maximization algorithm, and the optimal number of clusters was determined by minimizing the Bayesian Information Criterion (BIC). SNPs were assigned to the cluster with the highest membership probability without imposing a strict threshold, thereby retaining more variants for downstream analyses. The algorithm also quantifies the average causal effect of each cluster, termed the cluster mean.

For the overall variant set and each cluster, we performed conventional two-sample inverse-variance weighted (IVW) MR [21] for comparison with MR-Clust cluster means. Sensitivity analyses—MR-Egger regression [22], weighted median [23], and weighted mode [24]—assessed the robustness of cluster-specific estimates and horizontal pleiotropy (MR-Egger intercept test). Because clustering partitions instruments by their effects on both BMI and depression, cluster-specific SNP sets may be especially susceptible to correlated pleiotropy; we therefore additionally applied Causal Analysis Using Summary Effect Estimates (CAUSE), which models both correlated and uncorrelated pleiotropy using genome-wide summary statistics [25].

To characterize the biological relevance of each cluster, cluster-specific gene mapping and pathway enrichment analyses were performed using FUMA [26]. SNPs assigned to each cluster were mapped to genes via positional and eQTL mapping (SNP2GENE), and the resulting cluster-specific gene sets were tested for enrichment in Gene Ontology biological processes, KEGG pathways, and tissue-specific gene expression (GENE2FUNC), with Benjamini–Hochberg FDR correction for multiple testing. Cluster-specific gene sets were further compared with previously published BMI subtype clusters to assess convergence with established adiposity subtypes.

Polygenic risk score construction and validation in UK Biobank

The UK Biobank is a large, prospective cohort study. We included 472,374 participants of European descent, excluding individuals with inconsistent self-reported and biological sex, ten or more third-degree relatives, polyploidy, or missing genetic data (N = 14,445), yielding an analytic sample of 457,929 with complete genotype data. For each of the four genetic clusters previously identified using MR-Clust, we independently constructed a cluster-specific polygenic risk score (PRS) in the UK Biobank cohort. Each PRS was calculated as the weighted sum of the number of effect alleles carried by each individual, with weights corresponding to the effect sizes derived from the BMI GWAS summary statistics for the SNPs assigned to the respective cluster: $PRSi = \sum_{\mathrm{J}=1}^{\mathrm{M}} \beta_{\mathrm{j}} \mathrm{G}_{\mathrm{ij}}$. A higher cluster-specific PRS indicated stronger genetically proxied BMI exposure through the corresponding biological pathway. SNP-level details, R^2, and F-statistics for each PRS are provided in Supplementary Table 1. Depression was ascertained from ICD-10 diagnoses (F32–F33), Read Codes (versions 2 and 3) [27], and the UK Biobank mental health questionnaire (MHQ) [28], consistent with our previously validated approach [29]. The association between each cluster-specific PRS and depression risk was assessed using restricted cubic

splines (RCS) and logistic regression models, adjusting for age, sex, assessment centre, genotyping batch, and the first ten genetic principal components.

Plasma proteomics and brain IDPs data sources and mediation MR analysis

The UK Biobank Pharma Proteomics Project (UKB-PPP) characterizes the plasma proteomic profiles of 54,219 UK Biobank participants. Comprehensive protein quantitative trait loci (pQTL) mapping was conducted for 2,923 proteins, identifying 6,194 cis-pQTLs corresponding to 1,984 plasma proteins. Cis-pQTLs were defined as genetic variants located within ± 1,000 kb of the transcription start site of the gene encoding the corresponding protein, selected at genome-wide significance (P < 5E-08), with LD clumping (r^2 < 0.001 within a 10,000 kb window) applied to ensure IVs independence.

Summary statistics for the brain IDPs originated from a recently published GWAS conducted by Elliott et al., which examined 3,935 brain IDPs in a sample size of up to 33,224 individuals drawn from UK Biobank cohorts [30]. All findings are accessible via the Oxford Brain Imaging Genetics web browser (http://big.stats.ox.ac.uk/). Given the relatively limited number of genome-wide significant variant, a relaxed significance threshold of P <1E-05 was applied for IDP instrument selection, with the same LD clumping criteria (r^2 < 0.001 within a 10,000 kb window) applied to ensure independence.

To evaluate the mediating role of the plasma proteome in the pathway linking BMI-associated genetic clusters to depression, we implemented a two-stage MR framework based on cis-pQTLs. First, cis-pQTLs were used as IVs to estimate the causal effect of each plasma protein on depression risk; proteins showing a significant effect (FDR < 0.05) were retained. Colocalization analysis of these first-stage associations was performed using conventional Bayesian colocalization (coloc) and SuSiE-based colocalization (coloc.susie) [31]. A posterior probability of hypothesis 4 (PPH4) > 50% was considered moderate evidence and PPH4 > 70% strong evidence of colocalization. Second, we assessed the causal effect of each BMI cluster on each retained protein, again with FDR correction. A protein was considered a candidate mediator if the cluster exerted a significant effect on its level (FDR < 0.05) and the direction was concordant with the protein's effect on depression. As the two stages relied on distinct instrument sets, formal mediation proportions were not estimated; candidate mediators were defined by significance at both stages plus directional concordance.

For brain IDPs, we applied the conventional two-step MR approach (25). First, we estimated the causal effect of each IDP on depression risk (FDR-corrected); IDPs nominally associated with depression (P < 0.05) were retained. Second, we evaluated the causal effect of each BMI cluster on these depression-associated IDPs (FDR-corrected); IDPs with a nominally significant cluster-to-IDP effect (P < 0.05) directionally consistent with a plausible causal chain were retained as candidate mediators. For each candidate, the proportion of the total cluster effect mediated by the IDP was estimated, and an IDP was confirmed as a mediator if this mediation proportion was statistically significant (P < 0.05).

RESULTS

Genetic clustering identifies four mechanistically distinct pathways linking BMI to depression

Using BMI and depression GWAS, we identified 433 independent, genome-wide significant SNPs associated with BMI after quality control, harmonization, and Steiger filtering (Supplementary Table 1). Application of the MR-Clust algorithm to these instruments, based on their joint associations with BMI and depression risk, resolved this set into four substantive clusters (C1–C4), comprising 160, 55, 80, and 138 SNPs, respectively (Fig. 2a and Supplementary Tables 2–5). SNP-specific genetic associations with BMI and depression revealed clearly distinguishable clustering patterns. Variants in C1 and C2 exhibited positive associations with both BMI and depression, falling along steeper and shallower positive slopes, respectively, whereas variants in C3 showed positive associations with BMI but negative associations with depression, falling along a slope of opposing sign. Variants in C4 showed comparatively weaker and more variable associations with depression relative to their effect on BMI, clustering closer to the null.

Using the full set of 433 BMI-associated instruments, conventional two-sample IVW MR demonstrated a modest positive causal effect of BMI on depression risk (OR = 1.10, 95% CI: 1.07–1.14, P = 2.82E-08), with directionally consistent estimates from MR-Egger, weighted media, and weighted mode methods (Fig. 2b). No significant directional pleiotropy was detected using the MR-Egger intercept test (P-pleiotropy = 0.678). However, Cochran's Q statistic revealed extreme heterogeneity among the 433 instruments (P-heterogeneity = 5.09E-80), indicating that this aggregate estimate likely reflects a mixture of divergent underlying causal effects rather than a single homogeneous pathway—providing the rationale for the cluster-specific analyses that follow (Supplementary Fig. 1).

Cluster-specific IVW MR analyses revealed markedly divergent effects of BMI-associated genetic variants on depression risk (Fig. 2b). C1 (high-risk; n = 159 SNPs after LD exclusion) showed the strongest risk-increasing effect (per 1kg/m2, OR = 1.70, 95% CI: 1.63–1.76, P = 4.01E-162), consistent across sensitivity analyses (P-pleiotropy = 0.160) (Supplementary Fig. 2). C2 (moderate-risk; n = 55 SNPs) showed a more modest risk-increasing effect (OR = 1.18, 95% CI: 1.13–1.23, P = 2.52E-15), similarly robust across sensitivity analyses (Supplementary Fig. 3). In contrast, C3 (protective; n = 80 SNPs) exhibited a substantial protective effect (OR = 0.61, 95% CI: 0.58–0.64, P = 5.07E-75), corroborated by weighted median and weighted mode estimators (Supplementary Fig. 4). Despite evidence of horizontal pleiotropy (P-pleiotropy = 7.83E-05), CAUSE supported a causal over a shared-factor model for C3 (P = 9.43E-47; causal-model OR = 0.61, 95% CI: 0.54–0.70), corroborating the protective effect (Supplementary Fig. 5). C4 (null; n = 138 SNPs) showed a weaker protective effect (OR = 0.94, 95% CI: 0.90–0.97, P = 3.62E-04), though this was not consistently significant across all methods, indicating a less robust signal. Within-cluster heterogeneity was minimal across all four clusters (all P-heterogeneity > 0.05).

Cluster-specific gene sets exhibited distinct tissue-expression patterns (Supplementary Fig. 6). C1 genes were significantly enriched among genes upregulated in multiple brain regions, including the frontal cortex, anterior cingulate cortex, cerebellum, hippocampus, and pituitary (Bonferroni-corrected $P < 0.05$); C3 genes showed a convergent but more restricted pattern, enriched only in the frontal cortex and hippocampus; no significant enrichment was detected for C2 or C4. Pathway analyses further distinguished the four clusters (Supplementary Fig. 7): C1 genes were enriched for glutamatergic synapse components (Schaffer collateral–CA1 synapse, adjusted $P = 0.020$) and Wnt/β-catenin signaling; C2 genes for glutathione-mediated detoxification and xenobiotic metabolism (adjusted $P < 0.05$); and C3 genes for synaptic transmission and plasticity, including cholinergic, glutamatergic, serotonergic, and GABAergic synapses and long-term potentiation (adjusted $P < 0.05$), with recurrent involvement of MAPK3, PLCB3, GNGT1, and ADCY9.

Cluster-specific polygenic risk scores largely validate MR-derived causal directions in the UK Biobank

To provide independent, individual-level validation of the cluster-specific causal signals identified through MR-Clust, we constructed cluster-specific BMI polygenic risk scores and examined their associations with depression in the UK Biobank (Fig. 2c, Supplementary Table 6 and Supplementary Fig. 8). Consistent with the strong risk-increasing effect identified for C1, the C1-PRS showed a strong, statistically robust, and approximately linear positive association with depression risk across its full range (P overall = 6.55E-49, P non-linear = 0.933). The C2-PRS also showed a significant positive association with depression risk (P overall = 7.16E-09), with significant nonlinearity suggesting a threshold-like dose-response pattern (P non-linear = 0.018). In line with the protective causal effect identified for C3, the C3-PRS demonstrated a significant, monotonically decreasing association with depression risk (P overall = 1.57E-06, P non-linear = 0.358), providing independent observational support for the protective direction inferred from MR. Given the instability of the C4 signal across MR sensitivity analyses and its directionally discordant association in PRS validation, C4 was considered to provide insufficient evidence of a causal effect on depression and was therefore excluded from mechanistic interpretation. These associations remained robust across three adjustment models and four depression case definitions (ICD-10, Read Codes V2/V3, MHQ, and their combination), with C1-PRS and C3-PRshowing consistent, statistically significant effects throughout (Supplementary Table 7).

Circulating protein mediators of cluster-specific effects on depression

Cis-pQTL-based MR analyses testing the causal effect of 2,923 plasma proteins on depression identified 47 proteins showing a significant causal association with depression risk after FDR correction (Fig. 3a and Supplementary Table 8). Proteins conferring increased depression risk (OR > 1) included FES, PRKAR2A, FKBPL, UBE2L6, and ZFYVE19, among others, whereas proteins associated with reduced

depression risk (OR < 1) included CD40, METAP1D, TXNDC9, USP28, and HSPB1. We next tested whether cluster-specific BMI-associated SNPs exerted causal effects on any of these 47 depression-associated proteins, applying FDR correction for the number of proteins tested within each cluster, in order to identify candidate proteomic mediators of the cluster-specific effects of BMI on depression (Fig. 3b).

For C1, four proteins were identified as candidate mediators, all showing directionally concordant effects consistent with a risk-increasing mediation pathway (Supplementary Table 9). Genetically predicted C1-driven BMI increase was associated with elevated levels of ANGPTL2 (β = 0.183, P-FDR = 0.006), MEP1B (β = 0.108, P-FDR = 0.006), and PHLDB1 (β = 0.142, P-FDR = 0.028), each of which was in turn associated with increased depression risk (ANGPTL2: OR = 1.29, P-FDR = 0.005; MEP1B: OR = 1.02, P-FDR = 0.007; PHLDB1: OR = 1.28, P-FDR = 0.014). Conversely, C1 was associated with decreased levels of VWC2L (β = −0.146, P-FDR = 0.024), which was itself associated with reduced depression risk (OR = 0.88, P-FDR = 0.022). For C2, three candidate mediators largely overlapped with those of C1 (Supplementary Table 10): C2 was associated with increased ANGPTL2 (β = 0.242, P-FDR = 5.10E-05) and MEP1B (β = 0.128, P-FDR = 0.002) and decreased VWC2L (β = −0.313, P-FDR = 6.1E-06), all directionally concordant with C1. Among these risk-increasing mediators, ANGPTL2 and VWC2L showed colocalization evidence with depression (PPH4 = 68.4% and 71.3%, respectively).

For C3, four proteins were identified as candidate mediators of its protective effect on depression, all following a consistent pattern (Supplementary Table 11): C3 was associated with increased levels of FURIN (β = 0.216, P-FDR = 0.031), HLA-E (β = 0.186, P-FDR = 0.031), HSPB6 (β = 0.178, P-FDR = 0.031), and PARP1 (β = 0.219, P-FDR = 0.031), each of which was in turn associated with reduced depression risk (FURIN: OR = 0.94, P-FDR = 0.043; HLA-E: OR = 0.92, P-FDR = 0.010; HSPB6: OR = 0.77, P-FDR = 0.033; PARP1: OR = 0.91, P-FDR = 0.006). Notably, FURIN showed strong colocalization evidence with depression (PPH4 = 83.2%), providing the most robust genetic support among all candidate mediators. For C4, a partially overlapping set of protein was similarly identified as candidate mediators at the MR level (Supplementary Table 12).

Brain imaging-derived phenotypes mediate cluster-specific effects on depression risk

We next examined whether any of the 3,935 brain IDPs—spanning 16 categories including cortical area, cortical thickness, resting-state functional MRI (rfMRI) connectivity, and white matter microstructure—mediated the cluster-specific effects on depression risk (Fig. 3a). Two-step MR first identified 303 IDPs nominally associated with depression (P < 0.05) (Fig. 3b and Supplementary Table 13), of which only left rostral middle frontal cortical volume survived multiple-testing correction (OR = 0.94, 95% CI: 0.92–0.97, P-FDR = 0.008).

For C1, 26 of the 303 depression-associated IDPs were nominally associated with C1 and 21 were directionally concordant with a mediating pathway (Fig. 3c and Supplementary Table 14); formal mediation analysis retained one—rfMRI connectivity (ICA100 edge 73). C1-driven BMI increase was

associated with enhanced connectivity at this edge (β = 0.140, P = 0.007), which was itself associated with increased depression risk (β = 0.067, P = 0.004), accounting for an estimated 1.8% of the total C1 effect (mediation proportion P = 0.045) (Fig. 3d). No robust neuroimaging mediator was identified for C2 (Fig. 3c).

For C3, 15 depression-associated IDPs were nominally associated with C3 and 7 were directionally concordant; one—right putamen T1-weighted signal intensity—showed a significant mediating effect (Supplementary Table 15). C3-driven BMI increase was associated with reduced putamen signal intensity (β = −0.256, P = 0.001), which was itself associated with reduced depression risk (β = −0.499, P = 5.07E-75), accounting for an estimated 2.1% of the total protective C3 effect (mediation proportion P = 0.014) (Fig. 4).

DISCUSSION

In this study, a clustering-based Mendelian randomization approach resolved the heterogeneous BMI–depression relationship into four mechanistically distinct genetic pathways—two risk-increasing (C1, C2), one protective (C3), and one unstable (C4)—with directions corroborated by cluster-specific PRS in the UK Biobank. Cluster-specific enrichment analyses further reinforced this divergence: C1 genes were enriched across multiple brain regions and in glutamatergic synapse and Wnt/β-catenin signaling, C2 genes converged on glutathione-mediated detoxification, and C3 genes were specifically enriched in the frontal cortex and hippocampus and in synaptic transmission and plasticity pathways. Notably, despite their opposite effects on depression, C1 and C3 genes were both enriched in overlapping brain regions, suggesting that divergent obesity–depression pathways operate within shared central circuits. These pathways carried discrete molecular and neuroimaging signatures: ANGPTL2, MEP1B, VWC2L and enhanced resting-state connectivity for the risk-increasing clusters, versus FURIN, HLA-E, HSPB6, PARP1 and reduced putamen signal intensity for the protective cluster.

The proteomic mediators identified for the risk-increasing clusters are biologically consistent with known links between adiposity, chronic low-grade inflammation, and depression pathophysiology. ANGPTL2, a shared mediator of both C1 and C2, is a secreted glycoprotein implicated in chronic inflammation and insulin resistance, and has been mechanistically linked to endothelial dysfunction and neuroinflammatory signaling in prior work [32–35]; MEP1B, a metalloendopeptidase involved in inflammatory substrate processing, points toward a similar mechanistic axis [36,37], The convergence of these two proteins across two independent risk-increasing clusters strengthens the plausibility of an inflammation-mediated route from obesity to depression. In contrast, VWC2L, a bone morphogenetic protein (BMP)-signaling modulator with putative neurotrophic activity [38,39], was decreased by both C1 and C2. Prior work has linked the VWC2 family to obesity-related cognitive decline [40], suggesting that reduced VWC2L may mark a shared neurotrophic vulnerability across obesity-related brain disorders. PHLDB1, a regulator of AKT signaling and neuronal plasticity [41,42], emerged as a C1-specific mediator

despite substantial C1–C2 proteomic overlap, suggesting engagement only under more pronounced genetically proxied adiposity—consistent with the stronger C1 PRS–depression association.

Conversely, the proteins mediating the protective effect of C3—FURIN, HSPB6, HLA-E, and PARP1—span a functionally distinct set of pathways, including proprotein convertase activity, cellular stress response, immune regulation, and DNA damage repair, respectively [43–46]. Emerging evidence, such as reduced FURIN mRNA expression in the brains of patients with Alzheimer's disease or schizophrenia, has implicated a crucial role for furin in the pathophysiology of neurodegenerative and neuropsychiatric disorders [43]. Notably, prior work has also shown that obesity states facilitate the cleavage of adipolin, presumably through upregulation of furin in adipose tissue, suggesting that FURIN may serve as a mechanistic bridge linking peripheral adipose signaling to central neuropsychiatric outcomes—consistent with its identification here as a mediator of the BMI-depression pathway [47]. PARP1, in turn, has been implicated in neuronal resilience to oxidative stress, raising the possibility that the C3 pathway confers protection through enhanced cellular stress tolerance rather than through simple attenuation of inflammatory signaling [48,49]. That these two sets of mediators are almost entirely non-overlapping suggests that risk-conferring and protective BMI-related genetic variation operate through fundamentally distinct molecular programs, rather than representing opposite ends of a single biological continuum.

The neuroimaging findings add a complementary, though quantitatively more modest, layer of mechanistic insight. The identification of right putamen signal intensity as a mediator of the protective C3 pathway is notable given the putamen's established role within basal ganglia circuits governing reward processing, motivation, and psychomotor function—domains centrally implicated in depressive symptomatology, particularly anhedonia and psychomotor retardation [50–52]. Similarly, the C1-specific mediator, resting-state functional connectivity at a discrete network edge, may reflect large-scale network dysconnectivity previously associated with mood disorders. However, the proportion of the total cluster effect explained by these neuroimaging mediators was considerably smaller than that attributable to circulating proteins, and no robust neuroimaging mediator was identified for C2.

Limitations

Several limitations should be acknowledged. First, this study was conducted exclusively in populations of European ancestry, limiting generalizability to other ethnic groups; replication in diverse populations, including those in which the underweight–depression association has been most extensively characterized, is warranted. Second, although MR-Clust, complementary sensitivity analyses, and CAUSE were employed to minimize horizontal pleiotropy, residual unmeasured pleiotropic effects cannot be entirely excluded, particularly given the pleiotropy detected for C3 under conventional MR-Egger testing. Third, the proteomic and neuroimaging mediation analyses relied on cis-pQTL instruments and cross-sectional GWAS measurements, respectively, which may not capture the temporal dynamics of protein expression or brain structure relative to BMI changes and depression onset; reverse causation or measurement-related biases cannot be ruled out. Fourth, the small mediation proportions of the

neuroimaging pathways and the limited power of the underlying brain-wide GWAS suggest that additional central mediators likely remain undetected; these findings should be interpreted as a lower-bound estimate of neuroanatomical contributions. Finally, depression as ascertained in the GWAS datasets is a heterogeneous clinical phenotype encompassing varying symptom profiles and severity, potentially masking further etiological heterogeneity within the identified clusters.

CONCLUSION

In conclusion, the genetic relationship between BMI and depression is not governed by a single causal pathway but reflects the coexistence of mechanistically distinct, directionally opposing processes, mediated by discrete circulating protein signatures and, to a lesser extent, brain phenotypes. These findings challenge the framing of obesity as uniformly depression-promoting and support a subtype-specific understanding of the obesity–depression relationship. The candidate mediators distinguishing risk-conferring from protective pathways lay the groundwork for precision-medicine approaches to depression risk stratification and intervention in obesity.

Declarations

DATA AVAILABILITY

This prospective cohort analysis was conducted using the UK Biobank Resource under approved project number 99231, with additional analyses made possible through the generous sharing of GWAS summary statistics.

CODE AVAILABILITY

All analyses were performed in R version 4.5.1 using publicly available packages (TwoSampleMR, MR-Clust, CAUSE, coloc/coloc.susie) and the FUMA web platform; no custom code beyond standard package workflows was generated.

AUTHOR CONTRIBUTIONS

Ming Chen: Methodology, Visualization, Writing – original draft. Shuo Zhen: Writing – review & editing. Weipeng Zhang: Methodology; Jian Mao: Writing – original draft. Huantao Ruan: Visualization. Cailan Hou: Supervision, Validation. Yong Liu: Funding acquisition, Supervision. Shiqun Chen: Conceptualization, Funding acquisition, Project administration, Supervision. Writing – review & editing. All authors approved the final version of the manuscript for submission. Haozhang Huang: Conceptualization, Formal analysis, Methodology, Visualization, Writing – original draft, Writing – review & editing.

FUNDING

This study was funded by National Science and Technology Major Project (No. 2025ZD0547601), National Natural Science Foundation of China (no.82270339 and no.82470531), and Guangdong Basic and Applied Basic Research Foundation (2026B0303000003).

COMPETING INTERESTS

None

ETHICS

The UK Biobank Study received approval from the National Information Governance Board for Health and Social Care in England and Wales, the Community Health Index Advisory Group in Scotland, and the North West Multicenter Research Ethics Committee (No. E-2006-043-1131). All participants gave written informed consent. All GWAS summary statistics were obtained and analyzed in compliance with the principles outlined in the Declaration of Helsinki.

References

1. Milaneschi, Y., Lamers, F., Berk, M. & Penninx, B. Depression Heterogeneity and Its Biological Underpinnings: Toward Immunometabolic Depression. *Biol Psychiatry* 88, 369–380 (2020). https://doi.org/10.1016/j.biopsych.2020.01.014
2. Monroe, S. M. & Harkness, K. L. Major Depression and Its Recurrences: Life Course Matters. *Annu Rev Clin Psychol* 18, 329–357 (2022). https://doi.org/10.1146/annurev-clinpsy-072220-021440
3. Global, regional, and national burden of 12 mental disorders in 204 countries and territories, 1990–2019: a systematic analysis for the Global Burden of Disease Study 2019. *Lancet Psychiatry* 9, 137–150 (2022). https://doi.org/10.1016/s2215-0366(21)00395-3
4. Wang, R.-Z. *et al.* Body weight in neurological and psychiatric disorders: a large prospective cohort study. *Nature Mental Health* 2, 41–51 (2024). https://doi.org/10.1038/s44220-023-00158-1
5. Endres, K. J. *et al.* Fasting ghrelin as mediator between obesity and depressive symptoms: a pre-registered study. *npj Mental Health Research* 5, 28 (2026). https://doi.org/10.1038/s44184-026-00217-2
6. Sheir, S., Piazza, G. G., Davies, N. M. & Pingault, J.-B. Genetic clusters of BMI reveal symptom-specific causal effects on depression. *Molecular Psychiatry* (2026). https://doi.org/10.1038/s41380-026-03830-x
7. Chen, M. *et al.* New insights on underlying shared genetic architectures and causality of underweight and depression in East Asian populations. *J Affect Disord* 380, 226–229 (2025). https://doi.org/10.1016/j.jad.2025.03.126
8. Jabeen, T. *et al.* Genetic susceptibility to depression and risk of cardiometabolic diseases: a systematic review and meta-analysis of 21 Mendelian randomisation studies. *EClinicalMedicine* 89, 103587 (2025). https://doi.org/10.1016/j.eclinm.2025.103587

9. Meng, X. *et al.* Multi-ancestry genome-wide association study of major depression aids locus discovery, fine mapping, gene prioritization and causal inference. *Nat Genet* 56, 222–233 (2024). https://doi.org/10.1038/s41588-023-01596-4
10. Kang, J. *et al.* Plasma proteomics identifies proteins and pathways associated with incident depression in 46,165 adults. *Sci Bull (Beijing)* 70, 573–586 (2025). https://doi.org/10.1016/j.scib.2024.09.041
11. Yang, C. *et al.* Mendelian randomization and genetic colocalization infer the effects of the multi-tissue proteome on 211 complex disease-related phenotypes. *Genome Med* 14, 140 (2022). https://doi.org/10.1186/s13073-022-01140-9
12. Zaghlool, S. B. *et al.* Revealing the role of the human blood plasma proteome in obesity using genetic drivers. *Nat Commun* 12, 1279 (2021). https://doi.org/10.1038/s41467-021-21542-4
13. Ishizuka, N. *et al.* Differential brain volume between obese and underweight cognitively normal older adults with frailty in the JPSC-AD. *Sci Rep* 15, 19702 (2025). https://doi.org/10.1038/s41598-025-04659-0
14. Schmaal, L. *et al.* ENIGMA MDD: seven years of global neuroimaging studies of major depression through worldwide data sharing. *Transl Psychiatry* 10, 172 (2020). https://doi.org/10.1038/s41398-020-0842-6
15. Foley, C. N., Mason, A. M., Kirk, P. D. W. & Burgess, S. MR-Clust: clustering of genetic variants in Mendelian randomization with similar causal estimates. *Bioinformatics* 37, 531–541 (2021). https://doi.org/10.1093/bioinformatics/btaa778
16. Mutie, P. M., Stojanovic, T., Lo Faro, V., Karlsson, T. & Johansson, Å. Genetic and molecular signatures highlight diverse pathways linking obesity to type 2 diabetes. *Nat Commun* 17 (2026). https://doi.org/10.1038/s41467-026-74675-9
17. Skrivankova, V. W. *et al.* Strengthening the Reporting of Observational Studies in Epidemiology Using Mendelian Randomization: The STROBE-MR Statement. *Jama* 326, 1614–1621 (2021). https://doi.org/10.1001/jama.2021.18236
18. Skrivankova, V. W. *et al.* Strengthening the reporting of observational studies in epidemiology using mendelian randomisation (STROBE-MR): explanation and elaboration. *Bmj* 375, n2233 (2021). https://doi.org/10.1136/bmj.n2233
19. Yengo, L. *et al.* Meta-analysis of genome-wide association studies for height and body mass index in ~700000 individuals of European ancestry. *Hum Mol Genet* 27, 3641–3649 (2018). https://doi.org/10.1093/hmg/ddy271
20. Trans-ancestry genome-wide study of depression identifies 697 associations implicating cell types and pharmacotherapies. *Cell* 188, 640–652.e649 (2025). https://doi.org/10.1016/j.cell.2024.12.002
21. Burgess, S., Scott, R. A., Timpson, N. J., Davey Smith, G. & Thompson, S. G. Using published data in Mendelian randomization: a blueprint for efficient identification of causal risk factors. *Eur J Epidemiol* 30, 543–552 (2015). https://doi.org/10.1007/s10654-015-0011-z

22. Bowden, J., Davey Smith, G. & Burgess, S. Mendelian randomization with invalid instruments: effect estimation and bias detection through Egger regression. *Int J Epidemiol* 44, 512–525 (2015). https://doi.org/10.1093/ije/dyv080
23. Bowden, J., Davey Smith, G., Haycock, P. C. & Burgess, S. Consistent Estimation in Mendelian Randomization with Some Invalid Instruments Using a Weighted Median Estimator. *Genet Epidemiol* 40, 304–314 (2016). https://doi.org/10.1002/gepi.21965
24. Hartwig, F. P., Davey Smith, G. & Bowden, J. Robust inference in summary data Mendelian randomization via the zero modal pleiotropy assumption. *Int J Epidemiol* 46, 1985–1998 (2017). https://doi.org/10.1093/ije/dyx102
25. Morrison, J., Knoblauch, N., Marcus, J. H., Stephens, M. & He, X. Mendelian randomization accounting for correlated and uncorrelated pleiotropic effects using genome-wide summary statistics. *Nat Genet* 52, 740–747 (2020). https://doi.org/10.1038/s41588-020-0631-4
26. Watanabe, K., Taskesen, E., van Bochoven, A. & Posthuma, D. Functional mapping and annotation of genetic associations with FUMA. *Nat Commun* 8, 1826 (2017). https://doi.org/10.1038/s41467-017-01261-5
27. Brown, P. J., Warmington, V., Laurence, M. & Prevost, A. T. Randomised crossover trial comparing the performance of Clinical Terms Version 3 and Read Codes 5 byte set coding schemes in general practice. *Bmj* 326, 1127 (2003). https://doi.org/10.1136/bmj.326.7399.1127
28. Harshfield, E. L. *et al.* Association Between Depressive Symptoms and Incident Cardiovascular Diseases. *Jama* 324, 2396–2405 (2020). https://doi.org/10.1001/jama.2020.23068
29. Huang, H. *et al.* Sex-specific effects of depression on the incidence and risk factors for coronary heart disease: insights from multi-omics approaches. *Eur J Prev Cardiol* (2026). https://doi.org/10.1093/eurjpc/zwag363
30. Smith, S. M. *et al.* An expanded set of genome-wide association studies of brain imaging phenotypes in UK Biobank. *Nature neuroscience* 24, 737–745 (2021). https://doi.org/10.1038/s41593-021-00826-4
31. Chen, M. *et al.* Exploring the potential impact of TNF-α inhibition on major depressive disorder risk: Insights from a prospective cohort and genetic evidence. *Brain Behav Immun* 136, 106589 (2026). https://doi.org/10.1016/j.bbi.2026.106589
32. Kadomatsu, T., Endo, M., Miyata, K. & Oike, Y. Diverse roles of ANGPTL2 in physiology and pathophysiology. *Trends Endocrinol Metab* 25, 245–254 (2014). https://doi.org/10.1016/j.tem.2014.03.012
33. Thorin-Trescases, N., Labbé, P., Mury, P., Lambert, M. & Thorin, E. Angptl2 is a Marker of Cellular Senescence: The Physiological and Pathophysiological Impact of Angptl2-Related Senescence. *Int J Mol Sci* 22 (2021). https://doi.org/10.3390/ijms222212232
34. Yumoto, S. *et al.* Context-Dependent Roles of ANGPTL2-Mediated Inflammaging in Tissue Homeostasis, Pathological Tissue Remodeling, and Longevity. *Aging Cell* 25, e70370 (2026). https://doi.org/10.1111/acel.70370

35. Wu, Z. *et al.* CD146 is a Novel ANGPTL2 Receptor that Promotes Obesity by Manipulating Lipid Metabolism and Energy Expenditure. *Adv Sci (Weinh)* 8, 2004032 (2021). https://doi.org/10.1002/advs.202004032
36. Li, W. *et al.* Structural and functional properties of meprin β metalloproteinase with regard to cell signaling. *Biochim Biophys Acta Mol Cell Res* 1869, 119136 (2022). https://doi.org/10.1016/j.bbamcr.2021.119136
37. Arnold, P., Otte, A. & Becker-Pauly, C. Meprin metalloproteases: Molecular regulation and function in inflammation and fibrosis. *Biochim Biophys Acta Mol Cell Res* 1864, 2096–2104 (2017). https://doi.org/10.1016/j.bbamcr.2017.05.011
38. Miwa, H. *et al.* A novel neural-specific BMP antagonist, Brorin-like, of the Chordin family. *FEBS Lett* 583, 3643–3648 (2009). https://doi.org/10.1016/j.febslet.2009.10.044
39. Ohyama, Y. *et al.* Modulation of matrix mineralization by Vwc2-like protein and its novel splicing isoforms. *Biochem Biophys Res Commun* 418, 12–16 (2012). https://doi.org/10.1016/j.bbrc.2011.12.075
40. Margara-Escudero, H. J. *et al.* Plasma neurology-related proteins associated with cognition are modulated by lifestyle in adults. *EBioMedicine* 120, 105933 (2025). https://doi.org/10.1016/j.ebiom.2025.105933
41. Zhou, Q. L. *et al.* A novel pleckstrin homology domain-containing protein enhances insulin-stimulated Akt phosphorylation and GLUT4 translocation in adipocytes. *J Biol Chem* 285, 27581–27589 (2010). https://doi.org/10.1074/jbc.M110.146886
42. Hsu, Y. H. *et al.* Using brain cell-type-specific protein interactomes to interpret neurodevelopmental genetic signals in schizophrenia. *iScience* 26, 106701 (2023). https://doi.org/10.1016/j.isci.2023.106701
43. Zhang, Y. *et al.* The emerging role of furin in neurodegenerative and neuropsychiatric diseases. *Transl Neurodegener* 11, 39 (2022). https://doi.org/10.1186/s40035-022-00313-1
44. Secco, V. *et al.* HSPB6: A lipid-dependent molecular chaperone inhibits α-synuclein aggregation. *iScience* 27, 110657 (2024). https://doi.org/10.1016/j.isci.2024.110657
45. Gillespie, G. M., Quastel, M. N. & McMichael, A. J. HLA-E: Immune Receptor Functional Mechanisms Revealed by Structural Studies. *Immunol Rev* 329, e13434 (2025). https://doi.org/10.1111/imr.13434
46. Alemasova, E. E. & Lavrik, O. I. Poly(ADP-ribosyl)ation by PARP1: reaction mechanism and regulatory proteins. *Nucleic Acids Res* 47, 3811–3827 (2019). https://doi.org/10.1093/nar/gkz120
47. Enomoto, T. *et al.* Regulation of adipolin/CTRP12 cleavage by obesity. *Biochem Biophys Res Commun* 428, 155–159 (2012). https://doi.org/10.1016/j.bbrc.2012.10.031
48. Spiegel, J. O., Van Houten, B. & Durrant, J. D. PARP1: Structural insights and pharmacological targets for inhibition. *DNA Repair (Amst)* 103, 103125 (2021). https://doi.org/10.1016/j.dnarep.2021.103125
49. Lee, G. *et al.* SREBP1c-PARP1 axis tunes anti-senescence activity of adipocytes and ameliorates metabolic imbalance in obesity. *Cell Metab* 34, 702–718.e705 (2022). https://doi.org/10.1016/j.cmet.2022.03.010

50. Long, X. *et al.* Gray matter alterations in adolescent major depressive disorder and adolescent bipolar disorder. *J Affect Disord* 325, 550–563 (2023). https://doi.org/10.1016/j.jad.2023.01.049
51. Zheng, H. *et al.* The resting-state brain activity signatures for addictive disorders. *Med* 5, 201–223.e206 (2024). https://doi.org/10.1016/j.medj.2024.01.008
52. Bore, M. C. *et al.* Common and separable neural alterations in adult and adolescent depression - Evidence from neuroimaging meta-analyses. *Neurosci Biobehav Rev* 164, 105835 (2024). https://doi.org/10.1016/j.neubiorev.2024.105835

Figures

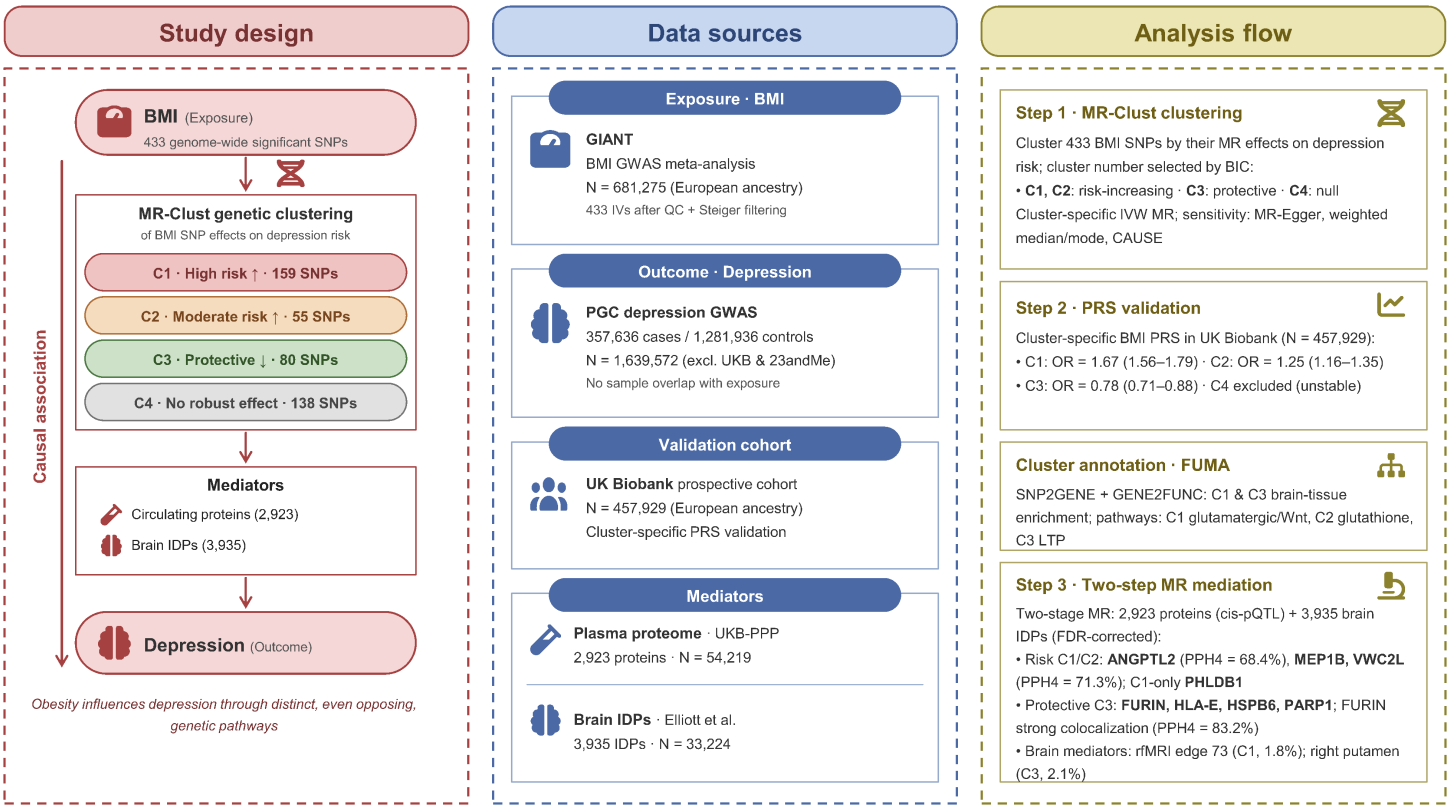


Figure 1

Study design overview. Abbreviations: BMI, body mass index; SNP, single-nucleotide polymorphism; MR, Mendelian randomization; IV, instrumental variable; IVW, inverse-variance weighted; BIC, Bayesian information criterion; CAUSE, Causal Analysis Using Summary Effect Estimates; PRS, polygenic risk score; OR, odds ratio; GIANT, Genetic Investigation of Anthropometric Traits; PGC, Psychiatric Genomics Consortium; UKB-PPP, UK Biobank Pharma Proteomics Project; IDP, imaging-derived phenotype; cis-pQTL, cis-protein quantitative trait locus; FDR, false discovery rate; MDD, major depressive disorder; rfMRI, resting-state functional magnetic resonance imaging.

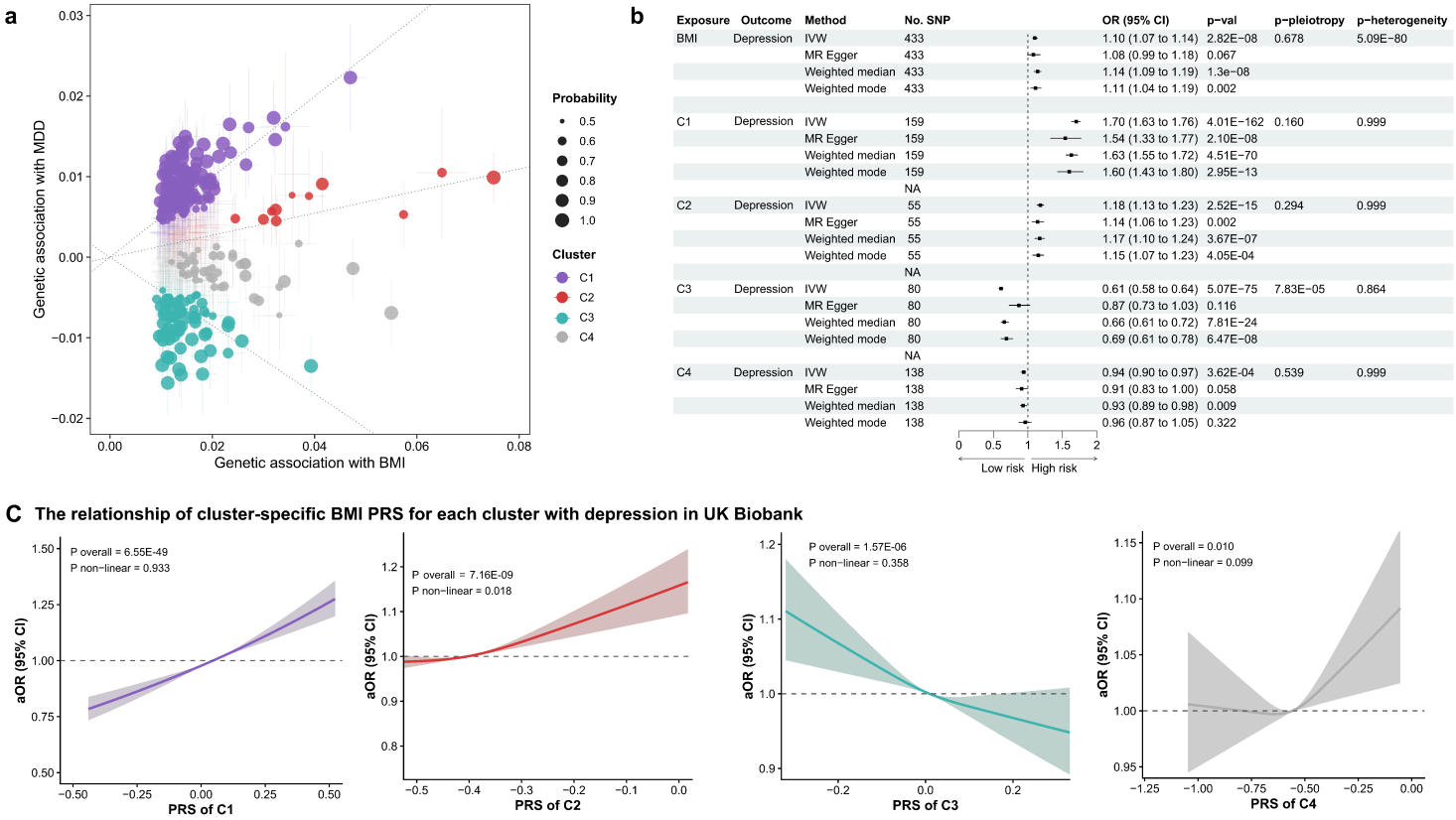


Figure 2

MR-Clust identifies four genetic clusters with divergent causal effects of BMI on depression, validated by cluster-specific PRS in the UK Biobank. (a) Scatter plot of SNP-level associations with BMI (x-axis) and depression (y-axis) for 433 BMI-associated instruments. Error bars denote SEs; point size reflects MR-Clust posterior probability. Colors indicate the four clusters: C1 (purple, n=160), C2 (red, n=55), C3 (teal, n=80), C4 (grey, n=138). Dotted lines show cluster-specific mean causal estimates. (b) Forest plot of MR estimates (IVW, MR-Egger, weighted median, weighted mode) for BMI on depression, overall and by cluster. No. SNP = instruments per analysis (C1: 159 after LD exclusion). OR, odds ratio; CI, confidence interval. P-pleiotropy, MR-Egger intercept test; P-heterogeneity, Cochran's Q test. (c) Restricted cubic spline plots of cluster-specific BMI-PRS vs. depression risk in the UK Biobank (N=457,929), adjusted for age, sex, assessment centre, genotyping batch, and top 10 genetic PCs. Lines show adjusted OR (aOR) relative to median PRS; shaded bands, 95% CI; dashed line, null (aOR=1.0). P overall, omnibus association test; P non-linear, test for non-linearity.

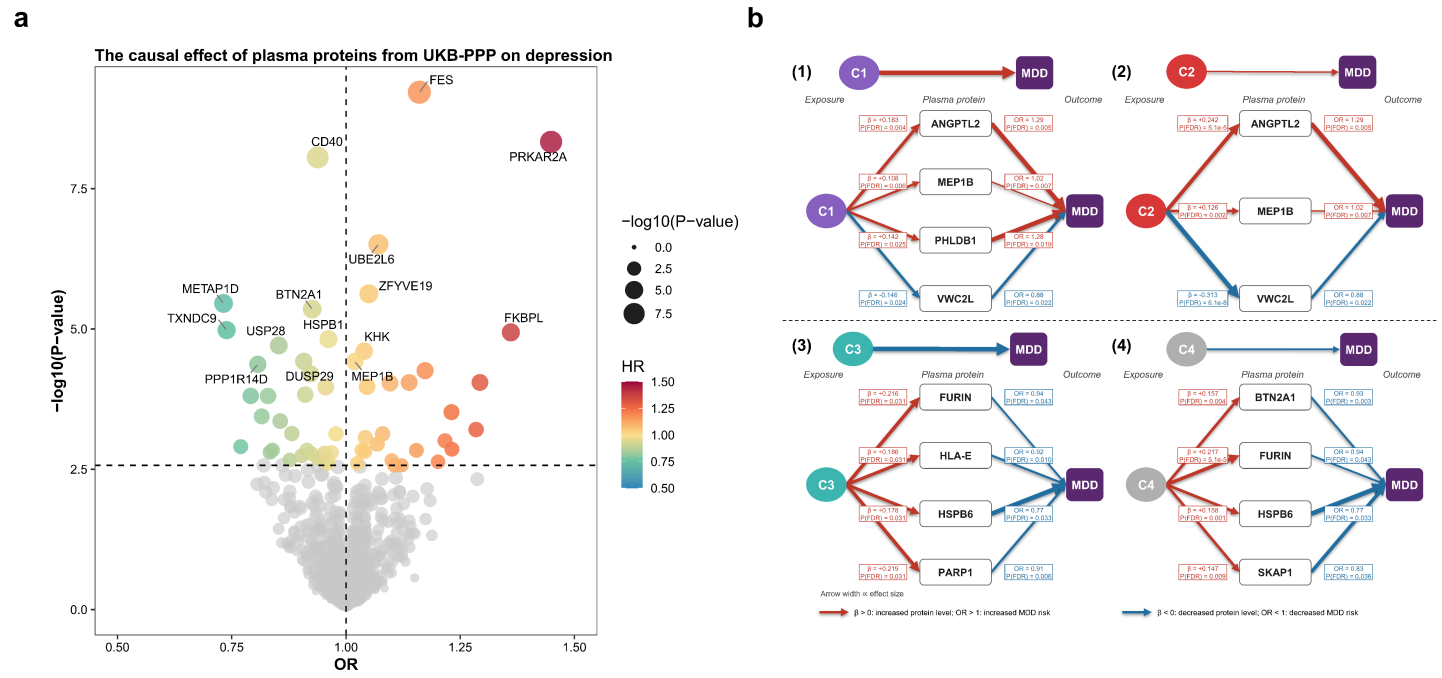


Figure 3

Circulating plasma proteins mediate cluster-specific effects of BMI on depression risk. (a) Volcano plot of cis-pQTL-based MR estimates for the causal effect of 2,923 plasma proteins (UKB-PPP) on depression. X-axis, odds ratio (OR); y-axis, $-\log_{10}(P)$; color, hazard ratio (HR) magnitude; point size, $-\log_{10}(P)$. Dashed line indicates the FDR < 0.05 significance threshold; 47 proteins survive correction (labeled selectively). (b) Two-step MR mediation diagrams for each cluster (C1–C4) linking BMI to depression via candidate protein mediators. Arrow width is proportional to effect size. Red arrows: β > 0 (increased protein level) or OR > 1 (increased MDD risk); blue arrows: β < 0 (decreased protein level) or OR < 1 (decreased MDD risk). β and P(FDR) denote the cluster→protein effect; OR and P(FDR) denote the protein→MDD effect. (1) C1; (2) C2; (3) C3; (4) C4.

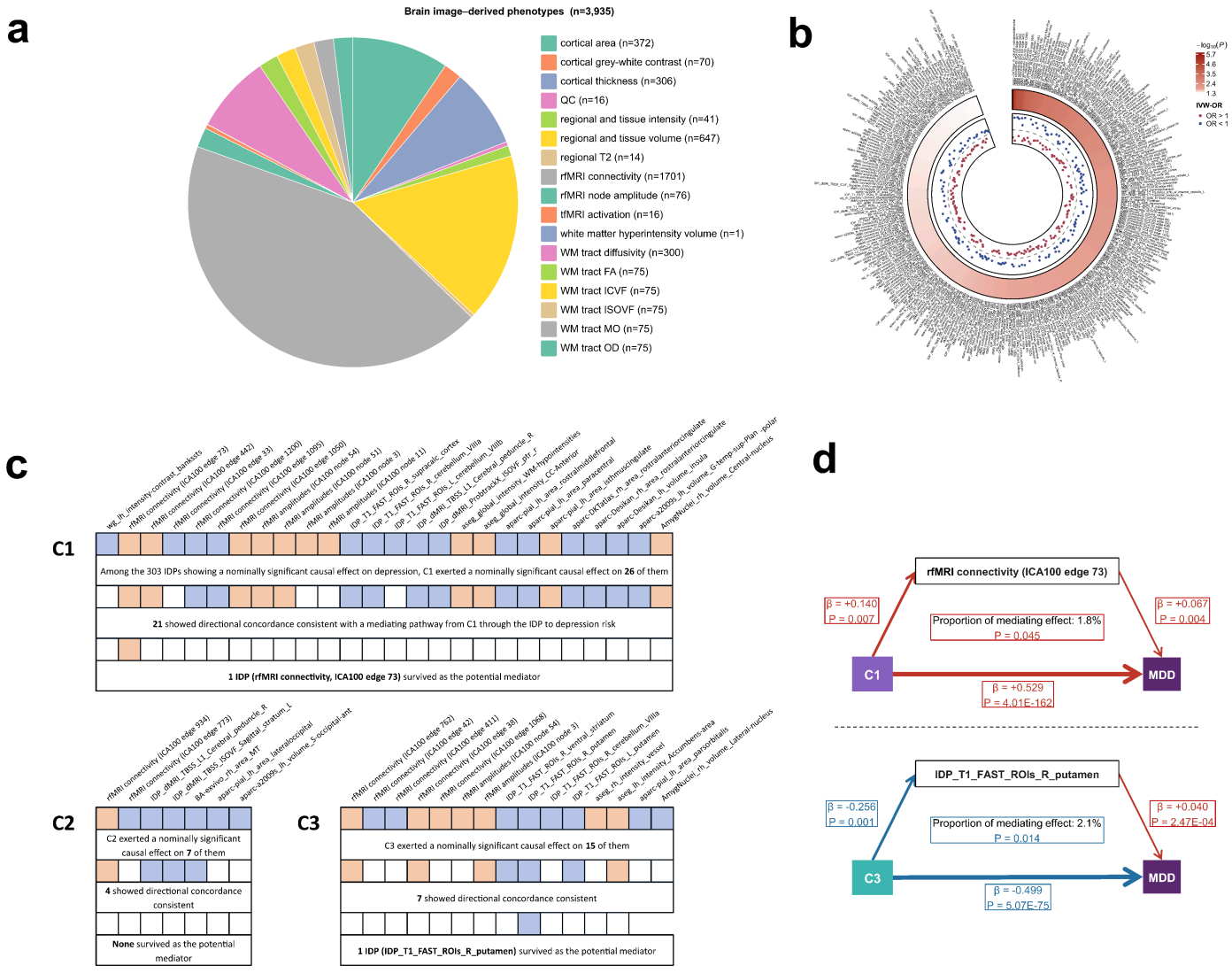


Figure 4

Brain imaging-derived phenotypes (IDPs) mediate cluster-specific effects of BMI on depression risk. (a) Pie chart of 3,935 brain IDPs analyzed, grouped into 16 categories (e.g., cortical area, cortical thickness, rfMRI connectivity, white matter [WM] tract metrics), with the number of IDPs per category indicated.

(b) Circular Manhattan plot of two-sample MR estimates for the causal effect of each IDP on depression, grouped by category (outer ring) and colored by $-\log_{10}(P)$ (inner heatmap). Red/blue points denote OR > 1 or OR < 1, respectively. (c) Two-step screening summary for C1–C3. Heatmap rows represent depression-associated IDPs ($P < 0.05$) showing a nominally significant causal effect of the corresponding cluster; colored cells (orange/blue) indicate directional concordance with a plausible cluster→IDP→depression mediating pathway. Text below each panel summarizes the number of IDPs retained at each screening step and the final mediator(s) confirmed by formal mediation testing. (d) Path diagrams for the two confirmed IDP mediators. Top: C1 → rfMRI connectivity (ICA100 edge 73) → depression (MDD). Bottom: C3 → right putamen T1-weighted signal intensity

(IDP_T1_FAST_ROIs_R_putamen) → MDD. Red arrows/values denote positive path coefficients (β); blue denote negative. Boxed values show the proportion of the total cluster effect on depression mediated by each IDP, with the corresponding mediation P value.

Supplementary Files

This is a list of supplementary files associated with this preprint. Click to download.

- SupplememtaryTable.xlsx
- SupplementaryFigure.docx
- ADDITIONALINFORMATIONinfo.docx